THE ASTROPHYSICAL JOURNAL, 238:969–981, 1980 June 15

SIMULTANEOUS ULTRAVIOLET, OPTICAL, AND X-RAY OBSERVATIONS OF THE X-RAY SOURCE VELA X-1 (HD 77581)

A. K. DUPREE,[1] H. GURSKY,[1] J. H. BLACK,[1] R. J. DAVIS, L. HARTMANN, T. MATILSKY, AND J. C. RAYMOND
Harvard-Smithsonian Center for Astrophysics

G. HAMMERSCHLAG-HENSBERGE AND E. P. J. VAN DEN HEUVEL[1]
University of Amsterdam

M. BURGER[2,3] AND H. J. G. L. M. LAMERS[1]
Astronomical Institute of Utrecht

P. A. VANDEN BOUT[1]
University of Texas

D. C. MORTON[1]
Anglo-Australian Observatory

C. DE LOORE[2]
Vrije Universiteit Brussel

E. L. VAN DESSEL
Royal Observatory, Belgium

J. W. MENZIES AND P. A. WHITELOCK
South African Astronomical Observatory

M. WATSON
University of Leicester

AND

P. W. SANFORD AND G. S. G. POLLARD
Mullard Space Science Laboratory

Received 1979 October 4; accepted 1979 December 27

ABSTRACT

Ultraviolet spectra of HD 77581, associated with the binary X-ray source Vela X-1, taken with the *International Ultraviolet Explorer* satellite (*IUE*) show a spectrum typical of an early B-type supergiant. However, the P Cygni profiles of strong resonance lines show substantial variations with orbital phase. These variations can be ascribed to the changing ionization state in the stellar wind caused by the X-ray emitting companion as suggested by Hatchett and McCray. The mass loss of the supergiant primary is determined to be $\sim 1 \times 10^{-6}\ M_{\odot}\ \mathrm{yr}^{-1}$. X-ray and spectroscopic and photometric optical observations, simultaneous with the *IUE* measurements, indicate behavior consistent with previous epochs. The interstellar spectrum shows strong, relatively broad lines of highly ionized Si IV and C IV which may result from the effects of X-rays upon the interstellar material neighboring the source.

Subject headings: stars: individual — ultraviolet: spectra — X-rays: binaries

I. INTRODUCTION

The X-ray source Vela X-1 (also known as 4U 0900 −40 and GX 263 + 3) was first detected by Chodil *et al.* (1967); the optical identification with HD 77581, a binary system containing a B0.5 Ib primary star, was established through the photometric period by Hiltner (1973), Vidal, Wickramasinghe, and Peterson (1973*a*, *b*), and Jones and Liller (1973). Subsequently, the system was shown to consist of a pulsar with a 283 s period (McClintock *et al.* 1976) that is orbiting the primary with a period of 8.96 days. The X-ray source is apparently formed by accretion of a massive stellar wind from the primary by the compact object. Because the X-ray pulsar velocity curve and the optical curve

[1] Guest Investigator with the *International Ultraviolet Explorer* satellite, which is sponsored and operated by the National Aeronautics and Space Administration, by the Science Research Council of the United Kingdom, and by the European Space Agency.

[2] Visiting Astronomer at the European Southern Observatory, La Silla, Chile.

[3] Recipient of an ESA Fellowship.

(van Paradijs *et al.* 1977) are well established, the masses and orbital parameters of this system are regarded as well known.

In this paper we report simultaneous observations of Vela X-1 in the X-ray, ultraviolet, and optical spectral regions. The X-ray monitoring was accomplished with the Sky Survey Instrument on board *Ariel 5* and the University College London instrument on board *Copernicus*. The program of optical photometry and spectroscopy was carried out at the South African Astronomical Observatory and the European Southern Observatory at La Silla, Chile. These collaborative efforts were initiated by the Guest Observers on the *International Ultraviolet Explorer* satellite (*IUE*) who obtained ultraviolet spectra of Vela X-1 during two 2-week periods that were dedicated by international agreement to observations of selected X-ray sources.

Since the star HD 77581 is of visual magnitude ~ 6.9, high-dispersion measurements are possible with *IUE*. Such observations permit examination of the detailed structure of the stellar wind, of the effects of the X-ray source upon the wind, and of the interstellar spectrum. Hatchett and McCray pointed out that an X-ray source embedded in a strong stellar wind could ionize a surrounding volume. The changing ionization might well be apparent in the P Cygni profiles of strong resonance lines formed in the expanding atmosphere. Although such behavior was not found in HD 153919, an Of star identified with the X-ray source 4U 1700 −37 (Dupree *et al.* 1978), HD 77581 is more likely to exhibit these effects because of the smaller optical depths of the strong resonance lines. We detect in this system, substantial phase effects in the changing profiles of selected P Cygni lines. Such behavior can also be inferred from low dispersion measurements of HDE 226868 (Cygnus X-1) as reported in Dupree *et al.* (1978) and Treves *et al.* (1980).

II. ULTRAVIOLET OBSERVATIONS

IUE spectra (Table 1) of HD 77581 were obtained at low dispersion (~ 6 Å resolution) and high dispersion (~ 0.1 Å resolution) from 1978 April 28 to May 5 and 1978 July 18 to July 23 during the collaborative periods; in addition, several spectra obtained on 1978 December 19 by some of us (A. K. D., L. W. H., and R. J. D.) are included. Details of the instrument and its performance can be found in Boggess *et al.* (1978*a*, *b*).

TABLE 1

IUE OBSERVATIONS OF HD 77581

Image[a]	JD Start Exp. (2,440,000+)	Exposure (min:sec)	Dispersion	Phase[b]	Notes
SWP 1433L	3627.32	1:48	Low	0.28	e, f
SWP 1433S	3627.33	5:0	Low	0.29	e, f
SWP 1441L	3628.56	1:48	Low	0.42	d, e, f
SWP 1441S	3628.57	5:0	Low	0.42	c, d, e, f
SWP 1442L	3628.71	180:0	High	0.44	c, e, f
SWP 1453L	3630.11	1:35	Low	0.60	e
SWP 1453S	3630.12	1:35	Low	0.60	e
SWP 1475L	3632.42	2:20	Low	0.85	c, e
SWP 1475S	3632.43	2:20	Low	0.85	c, e
SWP 1488L	3634.12	150:0	High	0.04	e
SWP 2087L	3712.99	125:0	High	0.84	
SWP 3648S	3862.45	5:00	Low	0.52	
SWP 3648L	3862.46	1:30	Low	0.52	
SWP 3649L	3862.49	150:0	High	0.52	
LWR 1412L	3627.35	0:40	Low	0.29	e, f
LWR 1412S	3627.36	4:00	Low	0.29	e, f
LWR 1417L	3628.58	0:40	Low	0.43	c, d, e, f
LWR 1417S	3628.60	4:00	Low	0.43	c, e, f
LWR 1418L	3628.80	70:0	High	0.45	c, e, f
LWR 1426L	3630.14	0:40	Low	0.60	e
LWR 1426S	3630.15	0:40	Low	0.60	e
LWR 1436L	3632.47	0:40	Low	0.86	c, e
LWR 1436S	3632.48	0:40	Low	0.86	c, e
LWR 1444L	3634.20	55:00	High	0.05	e
LWR 1847L	3707.96	60:00	High	0.28	
LWR 1878L	3713.06	42:00	High	0.85	

[a] L and S indicate large and small aperture, respectively.

[b] Phase 0.0 corresponds to X-ray eclipse at JD = 2,442,620.80 and $P = 8.964$ days (Watson and Griffiths 1977). Phase is calculated for mid-exposure.

[c] Simultaneous (within ± 0.2 JD) 12 Å mm^{-1} spectra obtained at ESO.

[d] Simultaneous (within ± 0.2 JD) 3.0 and 60 Å mm^{-1} spectra at SAAO.

[e] Simultaneous photometric observations at SAAO and/or ESO at La Silla, Chile.

[f] Simultaneous X-ray observations with *Ariel 5* or *Copernicus*.

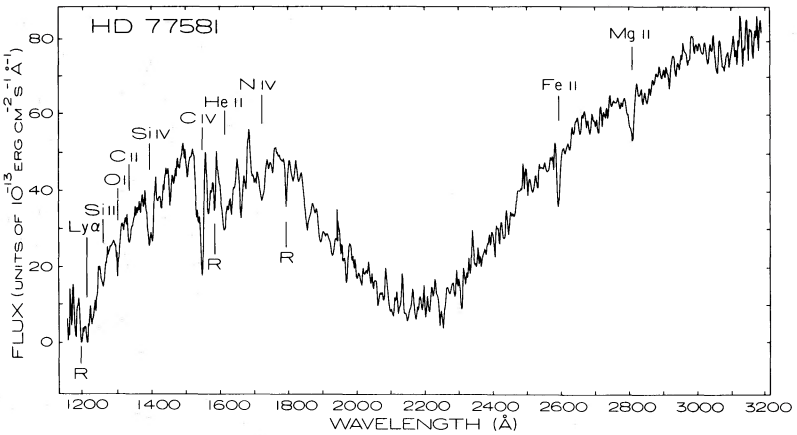

FIG. 1.—An average low dispersion spectrum of HD 77581 from 1150 to 3200 Å obtained by summing images at all phases. The absolute flux has been scaled to the measured flux at 1370 Å of 3.6×10^{-12} ergs cm^{-2} s^{-1} Å^{-1}. Line features at short wavelengths are found to vary with binary phase (see Fig. 2), although the continuum at 1370 and 1810 Å is constant to ~6%.

A composite low-dispersion spectrum is shown in Figure 1. The general appearance of the spectrum at low dispersion is similar to that of other early B supergiant stars. For instance, both HD 213087 (26 Cep), also a B0.5 Ib star, and κ Cas of spectral type B1 Ia show very similar features in spectra obtained with *IUE*. The low-dispersion spectra of HD 77581 are also like those of HDE 226868 (Cygnus X-1) as measured by *IUE* (Dupree *et al.* 1978; Treves *et al.* 1980), and the line features are commonly present in early type supergiants (see, for instance, Snow and Jenkins 1977). The long-wavelength region shows the 2200 Å extinction bump. Using the interstellar extinction curve of Nandy *et al.* (1976), we obtain $E_{B-V} = 0.7$, in agreement with the value derived by Vidal (1976).

a) Low Dispersion Spectra

In Figure 2 are shown individual low-dispersion short-wavelength spectra covering the region 1150–1950 Å.

It is apparent that the equivalent widths of many of the lines change with orbital phase; in particular the variation of the Si IV doublet near λ1400 is quite marked. The equivalent widths for C II, Si IV, and C IV for all the low-dispersion spectra taken with the small aperture are given in Table 2. The lines may be blended, so the wavelength range of the apparent features is given. The accuracy of the measurements can be inferred from the interstellar C II lines at λ1335 which have a total equivalent width of 1.58 ± 0.12 Å, suggesting that 1σ deviations in the equivalent width amount to ~10%. With this estimate of accuracy, it can be seen that Si IV has minimum equivalent width when the X-ray source is in front of the primary (phases 0.4 to 0.6) whereas any variation in C IV is commensurate with our estimated accuracy of measurement. This is consistent with the behavior of the high-dispersion spectra as discussed in the following section.

The continuum fluxes in two bands of 20 Å centered on λ1370 and λ1810 are listed in Table 2. These fluxes are in harmony with broad-band measures from the S2/68 Ultraviolet Sky Survey telescope in the *TD1* satellite (Nandy, Napier, and Thompson 1975). There is no variability on a level greater than the expected *IUE* photometric accuracy, ~6% at the 2σ level (Bohlin *et al.* 1980). This result is consistent with the optical data which show variations of $\lesssim$15% due to viewing the tidally distorted surface of the primary at

TABLE 2

EQUIVALENT WIDTHS AND FLUXES FROM LOW DISPERSION SPECTRA

	$\phi = 0.28$ SWP 1433S		$\phi = 0.42$ SWP 1441S		$\phi = 0.52$ SWP 3648S		$\phi = 0.60$ SWP 1453S		$\phi = 0.85$ SWP 1475S	
ION	$\Delta\lambda$(Å)	W_λ(Å)	$\Delta\lambda$(Å)	W_λ(Å)	$\Delta\lambda$(Å)	W_λ(Å)	$\Delta\lambda$(Å)	W_λ(Å)	$\Delta\lambda$(Å)	W_λ(Å)
C II	1329.0–1339.0	1.81	1328.6–1339.2	1.60	1327.8–1338.4	1.43	1329.0–1337.6	1.78	1331.1–1339.8	1.27
Si IV	1387.0–1397.8	3.49	1388.6–1397.2	2.16[a]	1383.6–1394.4	2.15[a]	1387.0–1347.8	3.04[a]	1387.0–1397.8	3.79
	1397.8–1406.4	2.71	1397.2–1405.8	1.53	1394.4–1406.4	1.60	1397.8–1406.4	1.97	1397.8–1406.4	2.86
C IV	1541.6–1554.6	6.59	1539.2–1554.2	6.74	1538.2–1553.2	5.94	1539.6–1554.6	7.80	1539.6–1554.6	6.55
F_λ[b] (1370)	3.6		3.7		3.5		3.5		3.7	
F_λ (1810)	4.2		4.3		4.4		4.1		4.3	

[a] Feature in blue wing of λ1393 line present, not included in W_λ.

[b] Average taken over 20 Å; flux is in units of 10^{-12} ergs cm^{-2} s^{-1} Å^{-1} from large aperture exposures.

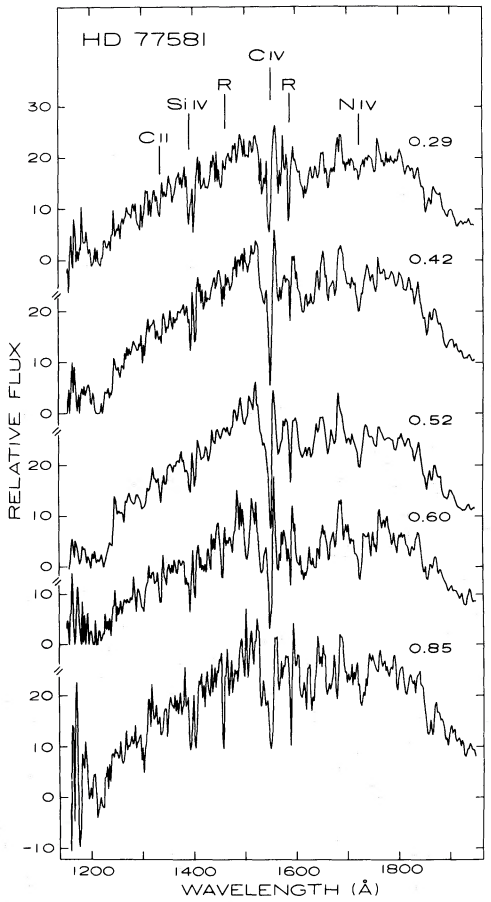

FIG. 2.—Low dispersion short wavelength spectra from 1150 to 1950 Å taken in small aperture. These spectra have been normalized to one another. Note that the shape of the continuum remains constant with phase; however, the strength of various absorption lines changes quite drastically with phase. This behavior is attributed to ionization of the stellar wind by the X-ray source.

varying aspects. At the phases of our low-dispersion observations, the optical variation is about 7% (Zuiderwijk *et al.* 1977*b*).

b) High Dispersion Spectra: Stellar Lines

At high dispersion, the strong P Cygni–shaped resonance lines of Si IV (λ1393.75 and λ1402.77) and C IV (λ1548.19 and λ1550.76) are very prominent. The N V resonance lines are extremely weak in these exposures due to the reddening of the star ($E_{B-V} = 0.7$) which reduces the flux at short wavelengths.

Here we concentrate on an analysis of the lines of Si IV and C IV, which show remarkable changes with orbital phase (see Figs. 3 and 4). At orbital phase $\phi = 0.04$, when the X-ray source is eclipsed, the Si IV lines have an edge velocity ~ 1700 km s^{-1}, showing little evidence of red P Cygni emission (Fig. 3). We assume the velocity at this phase to be comparable to the terminal velocity. This value is within the range found for other early B supergiant stars (Black *et al.* 1980). At $\phi = 0.44$, the edge velocity has been dramatically reduced to ~ 850 km s^{-1}, while the emission components have increased. At later phases, the absorption (blue) part of the lines appears to be made up of two components. The edge velocity remains the same at $\phi = 0.52$, but a broad absorption feature appears blueward of the λ1393 component, which extends to approximately the terminal velocity seen at $\phi = 0.98$. Similarly, the emission part of the λ1393 line appears to be depressed relative to the emission of the λ1402 lines, suggesting that absorption is present here as well. We therefore tentatively identify the broad absorption centered near λ1387.5 as high-velocity Si IV, near the terminal velocity of the undisturbed wind. In the low-dispersion spectra there is evidence of a blue wing component of λ1393 near $\phi = 0.5$ (Fig. 2), so this absorption may be a regular feature. By $\phi = 0.84$, the edge velocity has moved back out near the value for $\phi = 0.04$, and the emission has been reduced. The size of these changes in the edge velocity is consistent with the $\sim 30\%$ equivalent width variation seen in the low-dispersion spectra.

The variations observed here are qualitatively consistent with the model by Hatchett and McCray (1977) of the ionization of a stellar wind by an X-ray source. Near X-ray eclipse, the part of the wind producing the blueshifted P Cygni absorption will be unaffected by the X-rays, and thus the absorption part of the profile

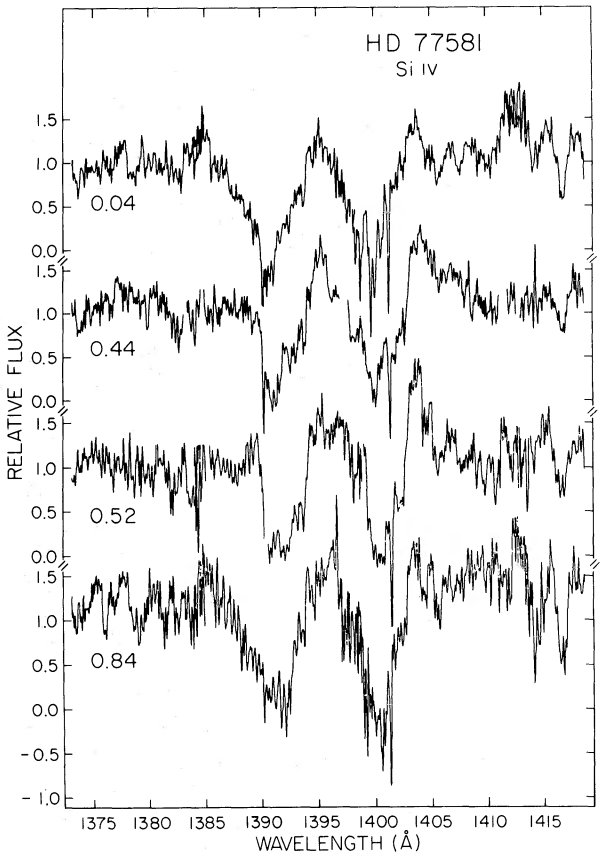

FIG. 3.—Si IV lines as a function of phase from high dispersion spectra. Note the substantial changes in the blue wing of both lines, and the appearance of a high velocity absorption feature at phase 0.52.

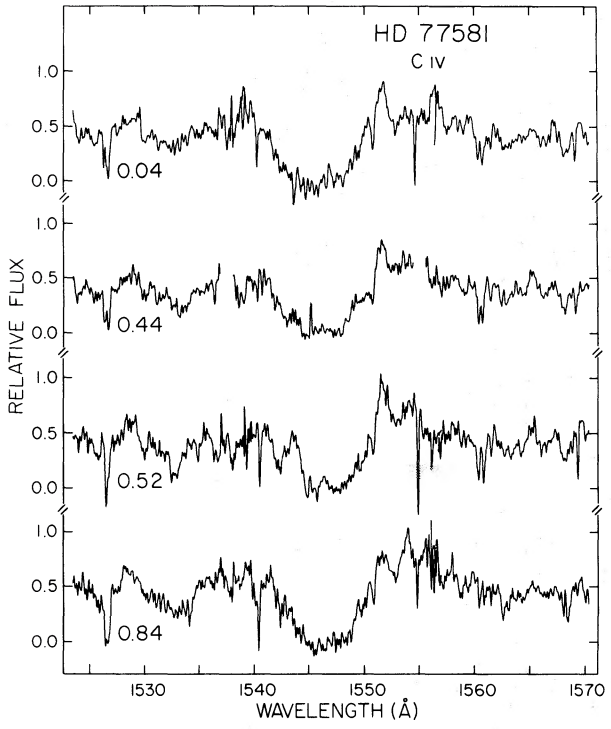

FIG. 4.—C IV lines as a function of phase from high dispersion spectra. The behavior of this profile is similar to that of Si IV.

should approximately represent the undisturbed stellar wind. The wind on the far side of the star, as seen from Earth, produces the P Cygni emission: at orbital phase $\phi = 0.04$, this gas is ionized by the X-ray source, reducing the emission. When the X-ray source is in front, near $\phi = 0.5$, the gas which produces the P Cygni absorption is now ionized to a higher state than before, resulting in the apparent reduction in the edge velocity, while the emission component is increased because the gas on the far side of the star, as seen from Earth, has returned to its normal state. The C IV line undergoes similar but less dramatic variations (Fig. 4). At $\phi = 0.04$, the edge velocity is ~ 1600 km s^{-1}, moving in to 1300 km s^{-1} at $\phi = 0.44$ and to 810 km s^{-1} at $\phi = 0.52$. The emission components change much less than those of Si IV. These data are consistent with the large optical depth of C IV than Si IV, indicating less sensitivity of the line profile to the X-ray ionization. A more detailed analysis of the line profile behavior will be presented in a later section.

c) *High Dispersion Spectra: Interstellar Lines*

Three high-dispersion *IUE* spectra of HD 77581, viz., SWP 1442, 1488, and 2087, have been examined for interstellar features. All three exposures were taken with the large aperture. Because the three exposures were obtained at different times and because the wavelength calibration of one was performed differently, the absolute wavelength scales differ. A system of narrow, interstellar absorption lines of C I, Cl I, and Ni II has been used to establish corrections to a common wavelength scale for the three exposures.

The high extinction toward HD 77581 is consistent with the rich interstellar absorption line spectrum. Equivalent widths of selected strong interstellar lines are presented in Table 3. The continuum levels have been established and the equivalent widths of the narrow lines have been measured using the techniques described in detail by Black *et al.* (1979). Of particular interest are the strong narrow interstellar lines of highly ionized species (C IV and Si IV) which are found toward another X-ray source 4U 1700−37 (HD 153919) (Dupree *et al.* 1978). These may reflect the influence of the X-ray source upon neighboring interstellar gas (cf. McCray, Wright, and Hatchett 1977). There is no evidence for the lines of N V in any of the spectra, but the signal levels are exceedingly low

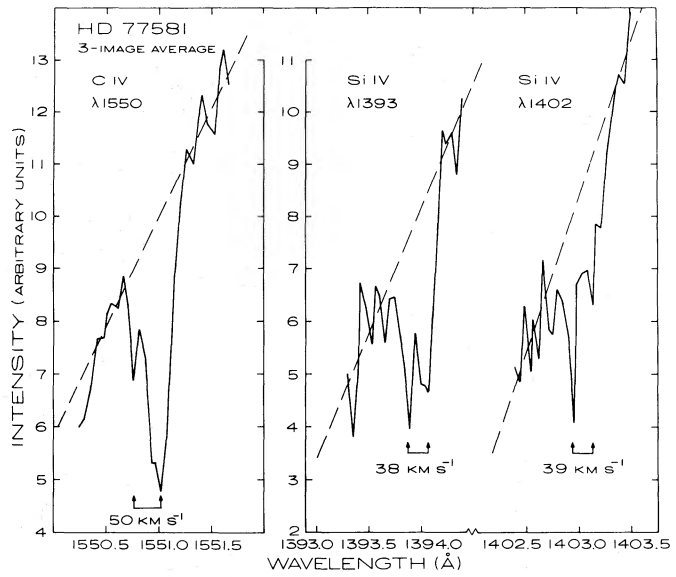

FIG. 5.—Interstellar lines of the high ionization species C IV and Si IV

TABLE 3

SELECTED INTERSTELLAR LINES: HD 77581

Species	Wavelength (Å)	W_λ(Å)
C I	1260.736	0.056
	1261.025+	0.064
	1261.520+	0.10
	1277.245	0.11
	1277.340+	0.03:
	1277.580+	0.10:
	1560.310	0.21
	1560.729+	0.18
	1561.423+	0.04:
	1656.266	0.21
	1656.928	0.24
	1657.380	0.15
	1657.907	0.15
C II	1334.532	0.48
	1335.703+	0.47
C IV	1548.188	(no signal)
	1550.762	0.172
N V	1238.808	(no signal)
	1242.796	(no signal)
O I	1302.169	0.39
Mg I	2025.824	0.14
Al III	1854.716	0.24
	1862.790	0.23
Si II	1260.421	0.17:
	1526.708	0.25
	1808.012	>0.16
Si IV	1393.755	0.137
	1402.770	0.110
S I	1474.005	0.072
	1474.390	0.085
	1807.341	0.080
S II	1259.520	0.10:
Cl I	1347.240	0.085
Cr II	2061.54	0.096
Fe II	1260.542	0.12:
	1608.456	0.097
Ni II	1741.547	0.11
Zn II	2025.512	0.19
	2062.016	0.099

NOTE.—A + sign designates the weighted, mean wavelength of a blend. Wavelengths in vacuum are tabulated below 2000 Å; wavelengths in standard air are listed above 2000 Å.

around 1240 Å, and upper limits to the line strengths are not meaningful. The λ1550 line of C IV appears clearly in all three spectra in the wing of the corresponding stellar feature. The equivalent width has been measured from the three-image average spectrum, and it is rather large. The λ1548 line of C IV is lost in the bottom of the stellar absorption. Both interstellar lines of Si IV are observed. The profiles of the interstellar C IV and Si IV lines are shown in Figure 5. The zero of the wavelength scale refers to the wavelength offset with respect to the interstellar lines of neutral and singly ionized species. The highly ionized species are at substantially the same radial velocity as the neutral and singly ionized species in this line of sight. The C IV and Si IV profiles exhibit distinct, blueshifted velocity components shifted by 35–50 km s^{-1} from the main features. In C IV, the structure in the profile can be seen in each of the three spectra individually. The equivalent widths tabulated in Table 3 are the total values for the entire profiles. In C IV, the main feature of the λ1550 line contributes about $W_\lambda = 0.143$ Å; the blueshifted component, about $W_\lambda = 0.029$ Å. Both lines of Si IV are observed; and if it is assumed that the total equivalent widths represent single velocity components, the doublet ratio implies a Doppler parameter $b = 9.8$ km s^{-1} and a column density N(Si IV) $= 5.4 \times 10^{13}$ cm^{-2}. The equivalent width of the λ1550 line of C IV corresponds to a column density N(C IV) $= 5.2 \times 10^{14}$ cm^{-2} if the Doppler parameter, $b = 9.8$ km s^{-1}, also applies to C IV.

The interstellar lines of C II have large equivalent widths. There are additional absorption features near λ1333 which, when combined with the C II lines, produce a total equivalent width at high dispersion in agreement with the low-dispersion values in Table 2.

III. X-RAY OBSERVATIONS

The *Ariel 5* Sky Survey Instrument (SSI) was used to make simultaneous measurements of the ~2–18 keV flux from Vela X-1 during the period 1978 April 12–30 continuously, and with patchy coverage to 1978 May 7. The light curves over this interval (Fig. 6) indicate that the X-ray behavior is similar to that found previously (Watson and Griffiths 1977; Charles *et al.* 1978) including eclipses lasting about 2 days, hour-to-hour variability, and "absorption dips." The X-ray data show good agreement with the extrapolated phase zero and period of Watson and Griffiths (1977) that we have adopted for this paper. The UCL X-ray instrument on board the *Copernicus* satellite observed Vela X-1 for 12 hours during the *IUE* collaborative period. Enlarged figures showing the correspondence with *IUE* observations (Figs. 7*a* and 7*b*) indicate that several *IUE* exposures—SWP 1441 (L and S) and LWR 1417 (L and S)—were centered on an absorption dip in the X-ray flux. As compared to SWP 1433 ($\phi = 0.28$) when the X-ray flux was greater by a factor of ~1.5 than SWP 1441 ($\phi = 0.42$), the UV broad-band fluxes at λ1370 and λ1810 are essentially constant. Thus the UV continuum appears to be dominated by the primary star, and effects of X-ray heating of the surface of the primary are not observed.

IV. OPTICAL MEASUREMENTS

a) Optical Photometry

Ground-based observations were made by M. B. and P. A. W. from 1978 April 25 to May 5 with the 1.0 m telescope at the South African Astronomical Observatory and from 1978 April 28 to May 2 with the 1.0 m telescope at ESO on La Silla, Chile. Strömgren *uvby* filters were used, supplemented with Hβ filters. Intercomparison of the measurements from both ob-

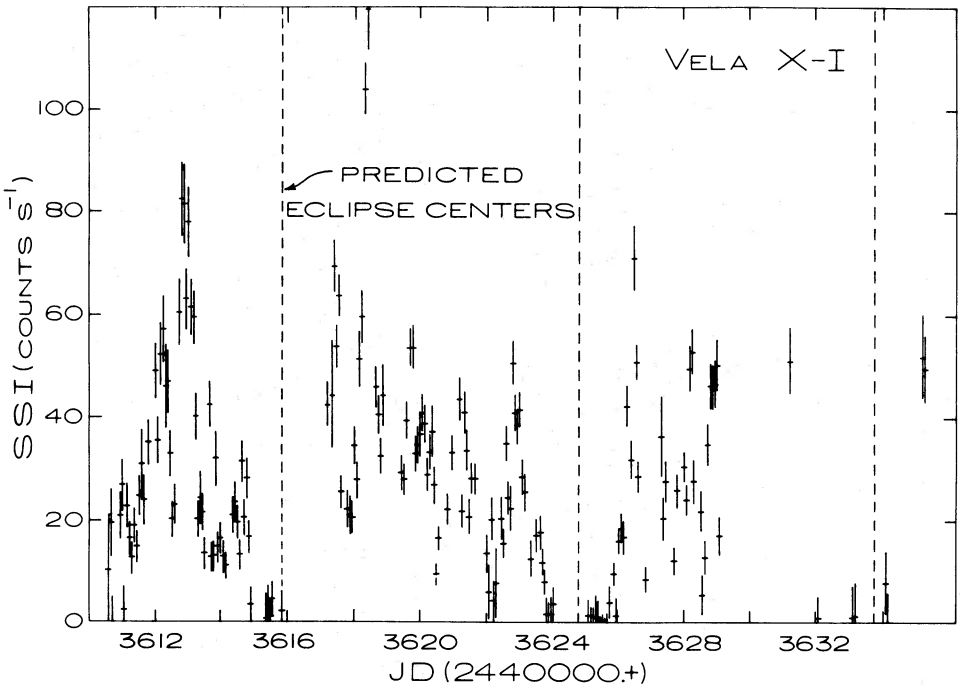

FIG. 6.—X-ray (2–10 keV) observations of Vela X-1 made with the *Ariel 5* SSI instrument during the collaborative period; the eclipse centers are predicted using the Watson and Griffiths (1977) ephemeris. One SSI count s^{-1} equals 5.1×10^{-11} ergs cm^{-2} s^{-1} in the 2–10 keV band.

servatories was made possible by observation of the same nonvariable comparison star, HR 3656.

During this period the variations in V were found to be very similar to the y-light curve determined by Zuiderwijk *et al.* (1977*a*, *b*), showing a double wave with a strong maximum at phase 0.25 and an amplitude of ~ 0.12 mag. No variation is evident in $\Delta(b - y)$, $\Delta(u - b)$, Δm_1, or the Hβ line. A search was made for short-period pulsations in the Hβ line. From 1.7 to 3.4 UT on 1978 May 2, HD 77581 was monitored with the Hβ filters using integration times of 9 s in both narrow (31.5 Å) and wide (185 Å) filters. One measurement of $\beta = -2.5 \log (H\beta_{narrow}/H\beta_{wide})$ resulted every 30 s. No variation of β was found either by averaging the data according to phase by assuming periods centered around 282.8916 s, or by computing a power spectrum and searching for peaks indicating periods between 60 and 5760 s. If any optical pulsation were present, the light variations have an upper limit of 0.005.

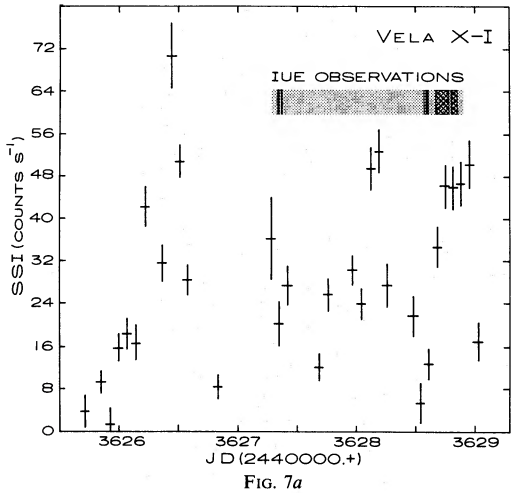

FIG. 7*a*

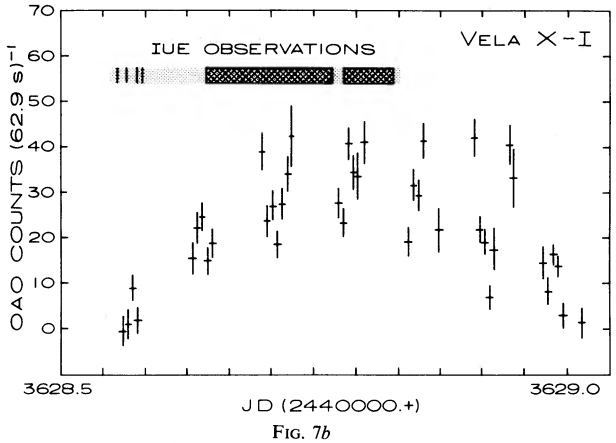

FIG. 7*b*

FIG. 7.—(*a*) An exploded view of the *Ariel 5* measurements that were simultaneous with the *IUE* exposures. One SSI count s^{-1} equals 5.1×10^{-11} ergs cm^{-2} s^{-1} in the 2–10 keV band. (*b*) *Copernicus* X-ray observations of Vela X-1 during the collaborative period. The *IUE* exposures that were simultaneous with the X-ray measurements are denoted by the heavy lines and crosshatched area. One OAO count per 62.9 s equals 3×10^{-11} ergs cm^{-2} s^{-1} in the 3–9.4 keV band.

b) Optical Spectroscopy

The image tube spectrograph was used by J. W. M. and P. A. W. on the 1.9 m telescope at the Sutherland station of the South African Astronomical Observatory to obtain spectra with dispersion of 30 Å mm^{-1} centered on λ4470 and 60 Å mm^{-1} centered at λ6130. The Hα profile is generally similar to those reported by Bessell, Vidal, and Wickramasinghe (1975) and references therein; as in their spectra, an absorption feature at ~ -400 km s^{-1} is absent near phases 0.4 to 0.5.

The coudé spectrograph attached to the 1.52 m telescope at ESO, La Silla, Chile, was used to obtain spectra at 12 Å mm^{-1} in the wavelength range 3800–4900 Å. Two of us (C. d. L. and E. L. vD.) report that the Hβ and He I λ4471 profiles are similar to those found at corresponding phases by Zuiderwijk, van den Heuvel, and Hensberge (1974). In particular the blue absorption present in both these lines near phase 0.5 is still found, indicating that such a periodic variation persisted over the time interval 1973–1978.

V. ANALYSIS OF MASS FLOW

In this section we deal with the implications of the high-dispersion spectra of Si IV and C IV in a more quantitative fashion.

The parameters for the Vela X-1 system have generally been adopted from Conti (1978). A list of observed and derived quantities is contained in Table 4. The inclination is greater than 74°; we adopt $i \sim 90°$ for simplicity. For the primary, for a spectral type of B0.5 Ib, Conti adopts $T_{\rm eff} = 26{,}000$ K; this value is consistent with the semiempirical effective temperatures derived for similar spectral types by Code *et al.* (1976). With a radius of 35 $R_\odot$, derived from the eclipse data, $L = 5 \times 10^5\ L_\odot$. The X-ray object is at a distance of about 1.5 R_* from the primary. The mass ratio is 12.3, with $M_1 \sim 22\ M_\odot$ and $M_x \sim 1.7\ M_\odot$ (van Paradijs *et al.* 1977). Our value of the terminal velocity of 1700 km s^{-1} is higher than the 950 km s^{-1} derived on the basis of Abbott's (1978) theory that the terminal velocity should be 3 times the escape velocity (corrected for continuum radiation pressure), but it agrees with the empirical relation between terminal velocity and escape velocity derived by Lamers, van den Heuvel, and Petterson (1976). Conti (1978) has noted that the derived stellar luminosity may be slightly too high. A downward revision to $2 \times 10^5\ L_\odot$, comparable to Cyg X-1, would yield a terminal velocity of 1380 km s^{-1} from Abbott's formula, in much better agreement with the data. The fact that the primary nearly fills its Roche lobe (Zuiderwijk *et al.* 1977*b*) may invalidate the usual velocity law.

Hatchett and McCray (1977) have evaluated the consequences of an X-ray source immersed in a stellar wind. Their calculations describe the primary effect of the X-rays—namely, ionization of certain regions in the wind. A secondary effect may be distortion of the velocity profile. We follow the Hatchett and McCray parametrization to predict the line profiles of Si IV and C IV as a function of orbital phase. First, it is necessary to know the velocity law and the mass loss rate. In principle these can be determined from the line profile. The task in Vela X-1 may be complicated by the fact that the wind (or the line-forming region) is not spherically symmetric. This we must ignore at present.

TABLE 4

ADOPTED AND DERIVED PARAMETERS FOR HD 77581

Quantity	Value	Notes and Reference
	Stellar Parameters	
Sp. type	B0.5 Ib	Conti 1978
$T_{\rm eff}$ (K)	26,000	Conti 1978
$E(B-V)$	0.7	This paper
L_* ($L_\odot$)	5×10^5	Conti 1978
L_x (ergs s^{-1})	10^{36}	Conti 1978
R_1 ($R_\odot$)	35	Conti 1978
M_1 ($M_\odot$)	22	van Paradijs *et al.* 1977
M_x ($M_\odot$)	1.7	van Paradijs *et al.* 1977
	Wind Parameters	
$V_{\rm terminal}$ (km s^{-1})	$\sim$1700	This paper from $\phi = 0.04$ observations of C IV and Si IV
$V_{\rm esc}$ (km s^{-1})	489	Assuming gravitational equilibrium
$V_{1.5R_*}$ (km s^{-1})	$\sim$860	This paper as inferred from $\phi = 0.52$ observations
$\dot{M}$ ($M_\odot$ yr^{-1})	$\sim 1 \times 10^{-6}$	This paper as derived from scaling to κ Cas and line profile fit
	Orbital Parameters	
i (degrees)	90	Conti 1978
Orbital period (days)	8.964	Watson and Griffiths 1977
Epoch of X-ray phase 0 (superior conjunction)	JD 2,442,620.80	Watson and Griffiths 1977

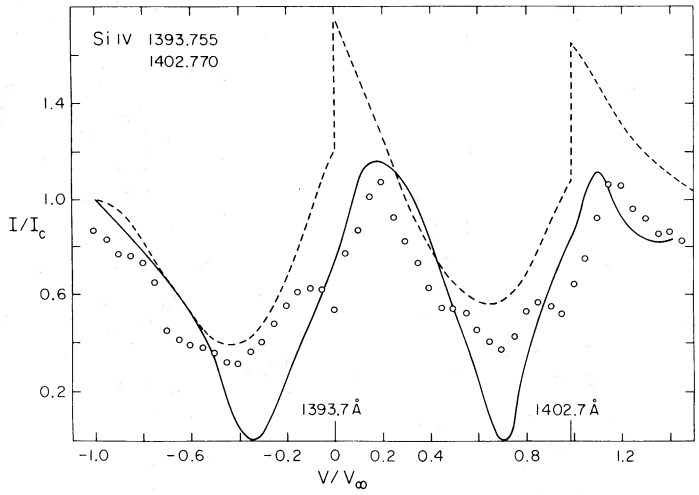

FIG. 8.—Theoretical and observed profile of the Si IV multiplet at phase 0.04. The solid line indicates the smoothed observed profile; the broken line denotes a profile from the Castor and Lamers (1979) atlas. The net profile after correcting for the underlying photospheric component is shown by open circles. The profile was calculated with $V_\infty = 1900$ km s^{-1}. If $V_\infty = 1700$ km s^{-1} had been adopted, as in the rest of this paper, the agreement at the blue edge of the profiles would be improved.

a) Estimate of Mass Loss and Velocity Law

To obtain a beginning estimate, line profiles are constructed for the Si IV multiplet at $\phi = 0.04$; this phase corresponds to X-ray eclipse, so that the blue side of the line profile should more nearly represent the undisturbed wind. The difficulty with obtaining mass loss rates from Si IV is that it is a minority species, and so the calculated $\dot{M}$ is a very sensitive function of the assumed ionization balance. The C IV line, on the other hand, is too saturated. Profile fits to the observed Si IV line at phase 0.04 are shown in Figure 8. Here theoretical profiles are taken from the atlas of Castor and Lamers (1979) with an added correction for the photospheric profile. From the profiles in Figure 8 a mass loss rate of $\dot{M} = 1 \times 10^{-6}\ M_\odot\ \mathrm{yr}^{-1}$ can be inferred, if the C IV and Si IV ionization fractions in the wind of HD 77581 are similar to those in the wind of τ Sco (B0 V) as found by Lamers and Rogerson (1978).

Additional theoretical profiles for HD 77581 were calculated independently by Olson (1979) using the Sobolev approximation, nonlocal radiative coupling (Rybicki and Hummer 1978), and a photospheric line contribution. Ionization equilibrium calculations for ϵ Ori (B0 Ia) and ζ Ori (O9.7 Ib) were used to establish the fractional concentration of Si IV in the atmosphere of HD 77581. These profiles suggest $\dot{M} \sim 0.6 \times 10^{-6}$ $M_\odot\ \mathrm{yr}^{-1}$.

Olson's profiles as well as those in Figure 8 differ from the observed profiles in several ways. First, the observed shape of the lines in HD 77581 is distinctly triangular and not as broad and rounded as the calculations or the observations of standard stars such as ϵ Ori, κ Cas (B1 Ia), or 26 Cep (B0.5 Ib). Moreover, the cores of the lines are deeper and occur at smaller values of v/v_∞ than the calculated profiles. Second, the blue wing of the observed profile is not well fitted either in Figure 8 where the opacity is larger than calculated or in Olson's results where the observed opacity is less than theory predicts. This emphasizes the uncertainties inherent in the ionization concentration and assumed velocity law as well as effects on the profile caused by photospheric lines.

The increased depth of the line cores might be an instrumental effect resulting from an overestimate of the background correction due to the close proximity of the individual echelle orders. However, several lines of evidence suggest that this is not the case. In the spectra of HD 77581, the absorption components of the P Cygni profiles of Si IV and C IV are approximately equal to zero and not negative as would result from an overcorrection of the background. The C II interstellar lines also reach zero (and not below). Moreover, an *IUE* spectrum of ζ Puppis shows agreement of central core intensity with that found by *Copernicus* (Morton and Underhill 1977).

A more attractive explanation of the deep central cores can result from the reduced intensity of the emission component of the P Cygni profile at phase 0.04. This would deepen the line cores and move the central minima to smaller values of v/v_∞. Consistent with this suggestion, two other early B supergiants that are not binary X-ray sources, ϵ Ori (Olson 1979) and 26 Cep, do not show such deep absorption in the cores of both lines.

The ionization structure of minority species is a difficult problem and influences the profile at high expansion velocities. Study of lines from several species could place some constraints on the temperature and ionization structure. In a system like HD 77581, moreover, the X-ray source influences the atmospheric ionization structure. The phase variation of the P Cygni profiles (see the following discussion) suggests that the ionized region of Si IV is confined to a volume

around the X-ray source. An increase in the level of X-ray flux, however, can substantially modify this geometry and can decrease Si IV at higher outflow velocities. It should be noted that Vela does show X-rays during eclipse of the pulsar (Becker *et al.* 1978), suggesting that scattered X-rays are present that may well affect the hemisphere of the wind facing Earth.

The mass loss rate can also be estimated by scaling from the B1 Ia star κ Cas. The infrared excess of κ Cas gives a well-defined result, assuming the velocity law is known. Barlow and Cohen (1977) found $\dot{M} = 1.4 \times 10^{-6} M_{\odot}$ yr^{-1} for κ Cas. Lamers, Paerels, and de Loore (1980) determined a better fitting velocity law which results in their mass loss rates being 1.8 times larger than the Barlow and Cohen values. After correcting for the difference in radii between HD 77581 (35 $R_{\odot}$) and κ Cas (45 $R_{\odot}$), and assuming the same ionization balance from the similarity of the two stars' spectra, we arrive at $\dot{M} \sim 2 \times 10^{-6} M_{\odot}$ yr^{-1}. This value is comfortably lower than the single-scattering luminosity limit $\dot{M} < L/(V_t c) = 6.6 \times 10^{-6} M_{\odot}$ yr^{-1}, and close to the value $\sim 1 \times 10^{-6} M_{\odot}$ yr^{-1} for other early B supergiants.

We adopt an empirical velocity relation: $V \approx V_{\infty}(1 - R_*/r)^{1/2}$ where R_* is the stellar radius, r the distance from the primary, and V_{∞} the terminal velocity of the wind. This implies a rather steep velocity gradient near the star as compared to most estimates (cf. Conti 1978), but is necessary if the velocity is to reach ~ 860 km s^{-1}, the observed velocity at $\phi = 0.53$, at a radial distance on the order of 1.5 R_* ($V = 860$ km s^{-1} at $r = 1.41\ R_*$).

b) Evaluation of Ionized Volumes

With this velocity relation and mass loss rate, two characteristic quantities of interest may be evaluated. First, the value of the column density of material from the stellar surface through the atmosphere is $\sim 2 \times 10^{22}$ cm^{-2}. Since the X-ray spectra require absorption with a column density between 3.7×10^{22} and 3.2×10^{23} cm^{-2} (Apparao and Chitre 1976), it appears that the wind can account for a significant fraction of the absorption. The other quantity is $\xi = L_x/nr_x^2$, where L_x is luminosity of the X-ray source, n the local number density of the gas, and r_x the distance measured from the X-ray source. The parameter ξ completely characterizes (for a given input spectrum) the ionization state in any local region of an optically thin gas (Tarter, Tucker, and Salpeter 1969). Hatchett and McCray (1977) have used ξ to describe the ionized volumes in the wind. They point out that the surfaces of constant column density from the X-ray source are roughly congruent to surfaces of constant ξ. Thus the surfaces of constant optical depth as measured from the X-ray source will be close to surfaces of constant ξ. As a first approximation we take these surfaces to exactly define the ionized volume in the wind. This may not be correct in detail; however, this assumption should indicate the general properties of wind ionization.

Using this approximation, we define $q\xi_0 = \xi$, where $\xi_0 = L_x/[n_x(1.5\ R_*)^2]$. Here n_x is the density of the stellar wind at the radial distance of the X-ray source from the primary. The ionization surfaces then can be parametrized by q (Hatchett and McCray 1977), and it remains to find the value of ξ and q at the boundaries of the optically thin region in C IV and Si IV.

For this we turn to calculations of the ionization structure produced by the X-ray emission. We adopt an input spectrum of bremsstrahlung with a 10 keV cutoff, and preliminary results from an improved and more detailed version of the Hatchett, Buff, and McCray calculations (Kallman and McCray 1979). The calculations are not only sensitive to the assumed X-ray spectrum but also to the ultraviolet spectrum, and predict fractional concentrations with an uncertainty of, say, a factor of 3. From the column density derived earlier, the average optical depth of the C IV lines in the atmosphere is estimated to be $\sim 4 \times 10^3 X_{\rm C\ IV}$, where $X_{\rm C\ IV}$ is the fraction of carbon in C IV. Therefore, when $X_{\rm C\ IV} \lesssim 10^{-4}$, $\tau \lesssim 0.4$ and the λ1550 lines will disappear. Inspecting the theoretical curves of Kallman and McCray (as an example, see Hatchett, Buff, and McCray 1976), we can find the values of ξ at which the fractional concentration of C IV equals 10^{-4} or less. Near the X-ray source, carbon is predominantly C VII. As the distance from the X-ray source increases, lower stages of ionization appear and the value of ξ decreases. Until C IV reaches an ionization fraction of $\sim 10^{-4}$, we assume that the resonance lines are optically thin. Hence the value of ξ at this point is used to define the boundary of the optically thin region. In the ionized volume interior to this, C IV is "absent." The region for C IV occurs for $\log \xi \gtrsim 1.7$. A similar calculation indicates that Si IV becomes optically thin for $X_{\rm Si\ IV} \lesssim 5 \times 10^{-4}$, which requires $\log \xi \gtrsim 1.2$. Using $L_X = 10^{36}$ ergs s^{-1} (Conti 1978), we find $\xi_0 = 21.4$, which places the ionization surfaces of C IV and Si IV at $q \approx 2.3$ and 0.75, respectively. The volume where C IV is absent is found (see Fig. 9) to be roughly a sphere lying along a line joining the primary and compact object, but centered at a greater distance than the X-ray source from the primary. Si IV is absent over a much larger extended volume that wraps around the primary star. The destruction of C IV over a smaller volume than Si IV follows naturally since higher energies are required to maintain the C IV ionization than for Si IV.

c) Calculation of the Line Profile

In order to investigate the predictions of the model, we have computed the absorption part of typical P Cygni profiles. Using the standard velocity law, we adopt a model for ionization of the ion in question by assuming that the fractional abundance is proportional to r^{-2}; the generalized profiles calculated by Olson (1978) indicate that this choice results in appropriate line shapes. We assume that within the q-surface the ion in question is completely destroyed. These assumptions result in the theoretical profiles shown in

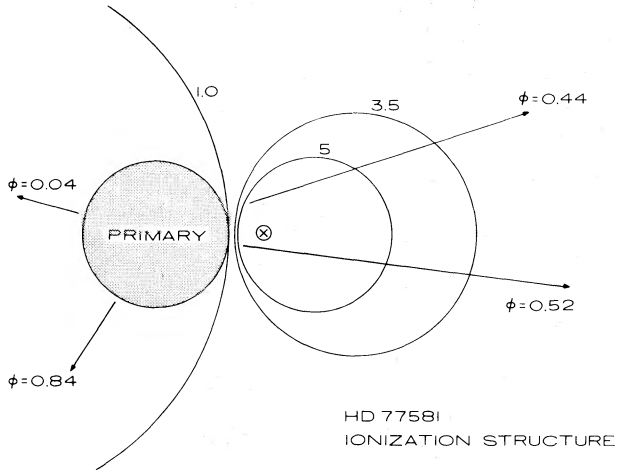

FIG. 9.—Predicted ionization surfaces for $q = 3.5$ and $q = 5$; within these spheres, it is assumed that an ion is missing from the volume to the right of the $q = 1$ locus. This figure and the profiles in Fig. 10 are calculated by assuming the eccentricity of the orbit, e, equals 0. With the parameters of Rappaport *et al.* (1976), $e = 0.13$, and the positions of the phase 0.44 and 0.52 are advanced by $\sim 7°$ in a clockwise direction; the profiles in Fig. 10 will show the same general features.

Figure 10. These calculations show overall agreement with the observed behavior of the C IV and Si IV lines. In particular, the narrow high-velocity feature that occurs at $\phi = 0.52$ is reproduced. The high-velocity feature does not appear for $q \lesssim 2$ corresponding to the Si IV profile at $\phi = 0.44$. Moreover, there is clearly more Si IV emission at $\phi = 0.44$ and 0.52 than at the other phases; the same effect is present in C IV, although to a lesser extent. This is consistent with the destruction of these species in a volume that extends beyond the occulting disk of the star. From these agreements we conclude that the ionization state in the wind is reasonably well understood.

There are discrepancies in details of the theoretical profiles when compared to the observations. For instance, the Si IV line exhibits high velocity absorption at $\phi = 0.52$, implying (see Fig. 9) that $q \gtrsim 2$. Such a value contradicts the observations at $\phi = 0.44$ and the derivation of q above. The implied increase in q can be achieved by a decrease in the X-ray luminosity. X-ray measurements taken simultaneously with the exposure at $\phi = 0.44$ show that the average flux was a factor of ~ 2 times higher than the flux at $\phi = 0.52$ during the two preceding cycles (see Fig. 6 and Figs. 7*a*, 7*b*). While we do not have simultaneous X-ray measurements for the spectrum at $\phi = 0.52$, it is plausible that the X-ray flux during the exposure at this phase was lower than at $\phi = 0.44$. A factor of 2 decrease would increase the q value and produce high velocity absorption. Because of the high densities in the wind, there is immediate response of the atmosphere to a varying X-ray flux. It may also be necessary to include the dynamical effects of the X-ray source on the wind in order to understand the detailed line profile behavior (MacGregor and Vitello 1980).

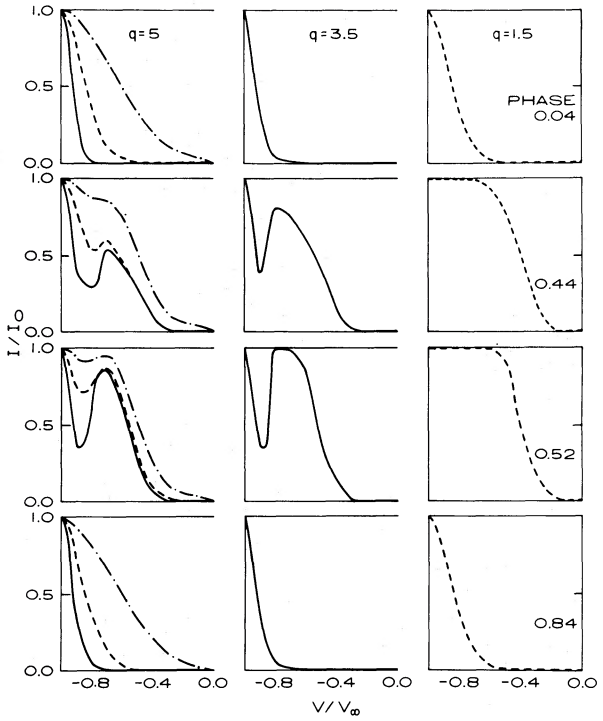

FIG. 10.—Calculated blue absorption wing of P Cygni profiles at four phases and for three values of q assuming the orbital eccentricity $e = 0.0$. The optical depth was set equal to three different values: 1 (*dot dash line*); 5 (*dashed line*); and 17 (*solid line*). Here the optical depth τ_z is defined where $VV_\infty^{-1} = 0.5$.

One further feature of the spectra deserves comment. An absorption component, centered at $\sim\lambda 1393.0$, appears in the Si IV line profile at $\phi = 0.44$ and 0.52. It is possible that this feature represents structure in the wind. However, Kamp (1976) has shown that the photospheric Si IV line profile is expected to be very strong in early B stars. Using his calculations, we have experimented with various line profiles. The results are sensitive to the assumed optical depth of the wind near the star. If the optical depth is not much greater than unity, the photospheric line can produce a net profile with a component similar to that observed. Additionally, the q-volume affects the shape of the blue emission component present in the P Cygni profile, an effect that was discussed earlier in the determination of the mass loss.

It is apparent that HD 77581 provides an exceptionally rich spectrum with which to investigate the physics of mass loss and the interplay between an X-ray source and a stellar atmosphere.

We conclude that the general behavior of the Si IV and C IV lines in the wind of Vela X-1 as a function of orbital phase can be understood in terms of the Hatchett and McCray (1977) model. A knowledge of the simultaneous value of the X-ray flux is essential to a self-consistent model. This is especially important for a variable source such as Vela X-1. The line profiles can change completely with a factor of 2 change in the X-ray flux. Such measurements constrain ξ as well. For

low ξ and q, the high-velocity absorption disappears. Similarly, for $q \gtrsim 10$, the high-velocity component tends to stand out too strongly at $\phi = 0.44$.

VI. DISCUSSION OF INTERSTELLAR LINES

The strong interstellar lines of highly ionized species found toward the X-ray sources HD 153919 (Dupree *et al.* 1978) and HD 77581 suggest that the X-ray source may be responsible. Assuming that Vela X-1 is a bremsstrahlung source of X-ray luminosity $L_x = 10^{36}$ ergs s^{-1} with a cutoff at 10 keV, and using the scaling laws of McCray, Wright, and Hatchett (1977), we predict that X-ray ionization can maintain column densities

$$N(\text{C IV}) = 5.25 \times 10^{13} n^{0.5} \text{ cm}^{-2}$$

and

$$N(\text{Si IV}) = 1.22 \times 10^{13} n^{0.46} \text{ cm}^{-2}$$

in the surrounding interstellar gas. The prediction for C IV is in harmony with the observations for an ambient density of $n = 2.5$ cm^{-3}. At that density, only one-third of the Si IV column density would be due to X-ray ionization. Black *et al.* (1980) have shown that a normal star of type B0.5 Ib can easily maintain the requisite additional amount of Si IV, 3.5×10^{13} cm^{-2}, in its H II region, but that a star this cool is unable to produce such a large column density of C IV. We suggest that the interstellar C IV is due primarily to X-ray ionization of the interstellar gas, while a large fraction of the Si IV may still arise in the more or less normal photoionized nebula associated with the primary of the binary system.

The blue velocity shift of the one interstellar component suggests that it might arise in a wind-driven "bubble" of the type envisaged by Weaver *et al.* (1977). However, we find that in order to obtain the column density observed in the blueshifted C IV, the ambient interstellar medium into which the bubble expands would need to have a density $\gtrsim 200$ cm^{-3}, for reasonable ages $\sim 10^6$ years. This extremely high density suggests that while the bubble expansion may account for the Doppler shift, the X-ray photoionization is the dominant production mechanism for C IV. For this picture to be acceptable, it is necessary that the photoionization front be outside the bubble; this occurs for ages less than 1.7×10^7 years, at a velocity ~ 46 km s^{-1}, according to the prescription of Weaver *et al.* (1977).

We are grateful to the individual sponsoring agencies, NASA, E.S.A., and the S.R.C. of the United Kingdom for the design and operation of such a versatile observatory. The individual staffs at NASA Goddard Space Flight Center and the Vilspa ground station of ESA were invaluable in giving advice and assistance in carrying out this observing program. R. McCray was most generous with discussion and helpful in providing unpublished results. We appreciate conversations and calculations of line profiles by G. Olson. H. Heinrichs offered substantive comments on the manuscript. S. Preston provided valuable assistance with the reduction of the spectra. This research was supported in part by NASA under grant NSG 5229 to the Harvard College Observatory, contract NAS 5-24332 to the Smithsonian Astrophysical Observatory, and grant NSG 5233 to the University of Texas. M. B. acknowledges the support of an ESA Fellowship.

REFERENCES

Abbott, D. C. 1978, *Ap. J.*, **225**, 893.
Apparao, K. M. V., and Chitre, S. M. 1976, *Space Sci. Rev.*, **19**, 281.
Barlow, M. J., and Cohen, M. 1977, *Ap. J.*, **213**, 737.
Becker, R. H., Rothschild, R. E., Boldt, E. A., Holt, S. S., Pravdo, S. H., Serlemitsos, P. J., and Swank, J. W. 1978, *Ap. J.*, **221**, 912.
Bessell, M. S., Vidal, N. V., and Wickramasinghe, D. T. 1975, *Ap. J. (Letters)*, **195**, L117.
Black, J. H., Dupree, A. K., Hartmann, L. W., and Raymond, J. C. 1980, *Ap. J.*, in press.
Boggess, A., *et al.* 1978*a*, *Nature*, **275**, 372.
Boggess, A., *et al.* 1978*b*, *Nature*, **275**, 377.
Bohlin, R. C., Holm, A. V., Savage, B. D., Snijders, M. A. J., and Sparks, W. M. 1980, *Astr. Ap.*, in press.
Castor, J., and Lamers, H. J. G. L. M. 1979, *Ap. J. Suppl.*, **39**, 481.
Charles, P. A., Mason, K. O., White, N. E., Culhane, J. L., Sanford, P. W., and Moffat, A. F. J. 1978, *M.N.R.A.S.*, **183**, 813.
Chodil, G., Mark, H., Rodrigues, R., Seward, F. D., and Swift, C. D. 1967, *Ap. J.*, **150**, 57.
Code, A. D., Davis, J., Bless, R. C., and Hanbury-Brown, R. 1976, *Ap. J.*, **203**, 417.
Conti, P. 1978, *Astr. Ap.*, **63**, 225.
Dupree, A. K., *et al.* 1978, *Nature*, **275**, 400.
Hatchett, S., and McCray, R. 1977, *Ap. J.*, **211**, 552.
Hiltner, W. A. 1973, *IAU Circ.*, No. 2502.
Jones, C., and Liller, W. 1973, *Ap. J. (Letters)*, **184**, L121.
Kallman, T., and McCray, R. 1979, private communications.
Kamp, L. W. 1976, NASA Tech. Rept. TRr-455.
Lamers, H. J. G. L. M., and Rogerson, J. B. 1978, *Astr. Ap.*, **66**, 417.
Lamers, H. J. G. L. M., van den Heuvel, E. P. J., and Petterson, J. A. 1976, *Astr. Ap.*, **49**, 327.
Lamers, H. J. G. L. M., Paerels, F. B. S., and de Loore, C. 1980, *Astr. Ap.*, in press.
MacGregor, K., and Vitello, P. 1980, in preparation.
McClintock, J. E., *et al.* 1976, *Ap. J. (Letters)*, **206**, L99.
McCray, R., Wright, C., and Hatchett, S. 1977, *Ap. J. (Letters)*, **211**, L29.
Morton, D. C., and Underhill, A. B. 1977, *Ap. J. Suppl.*, **33**, 83.
Nandy, K. M. D., Napier, D., and Thompson, G. I. 1975, *M.N.R.A.S.*, **171**, 259.
Nandy, K. M. D., Thompson, G. I., Jamar, C., Monfils, A., and Wilson, R. 1976, *Astr. Ap.*, **51**, 63.
Olson, G. 1978, *Ap. J.*, **226**, 124.
———. 1979, private communication.
Rybicki, G., and Hummer, D. 1978, *Ap. J.*, **219**, 654.
Snow, T. P., and Jenkins, E. B. 1977, *Ap. J. Suppl.*, **33**, 269.
Tarter, B. C., Tucker, W. H., and Salpeter, E. E. 1969, *Ap. J.*, **156**, 943.
Treves, A., *et al.* 1980, *Ap. J.*, in press.
van Paradijs, J., Zuiderwijk, E. J., Takens, R. J., Hammerschlag-Hensberge, G., van den Heuvel, E. P. J., and de Loore, C. 1977, *Astr. Ap. Suppl.*, **30**, 195.
Vidal, N. V. 1976, in *X-Ray Binaries*, ed. E. Boldt and Y. Kondo (NASA SP-389), p. 575.

Vidal, N. V., Wickramasinghe, D. T., and Peterson, B. A. 1973*a*, *IAU Circ.*, No. 2503.
———. 1973*b*, *Ap. J.* (*Letters*), **182**, L77.
Watson, M., and Griffiths, R. 1977, *M.N.R.A.S.*, **178**, 513.
Weaver, R., McCray, R., Castor, J., Shapiro, P., and Moore, R. 1977, *Ap. J.*, **218**, 377.
Zuiderwijk, E. J., Hammerschlag-Hensberge, G., van Paradijs, J., Sterken, C., and Hensberge, H. 1977*a*, *Astr. Ap. Suppl.*, **27**, 433.
———. 1977*b*, *Astr. Ap.*, **54**, 167.
Zuiderwijk, E. J., van den Heuvel, E. P. J., and Hensberge, G. 1974, *Astr. Ap.*, **35**, 353.

J. H. Black, R. J. Davis, A. K. Dupree, H. Gursky, L. Hartmann, and J. C. Raymond: Harvard-Smithsonian Center for Astrophysics, 60 Garden Street, Cambridge, MA 02138

M. Burger and H. J. G. L. M. Lamers: The Astrophysical Institute, Space Research Laboratory, Beneluxlaan 21, 3527 HS Utrecht, The Netherlands

C. de Loore: Astrophysical Institute, Vrije Universiteit Brussel, Pleinlaan 2, 1050 Brussel, Belgium

G. Hammerschlag-Hensberge and E. P. J. van den Heuvel: Astronomical Institute, University of Amsterdam, Roetersstraat 15, 1018WB, Amsterdam, The Netherlands

T. Matilsky: Physics Dept., Rutgers University, Serin Physics Laboratory, Piscataway, NJ 08854

J. W. Menzies and P. A. Whitelock: South African Astronomical Observatory, P. O. Box 9, Observatory, Cape 7935 South Africa

D. C. Morton: Anglo-Australian Observatory, P.O. Box 296, Epping, N.S.W. 2121, Australia

G. S. G. Pollard and P. W. Sanford: Mullard Space Science Laboratory, Holmbury St. Mary, Dorking, Surrey, England

P. A. Vanden Bout: Astronomy Department, University of Texas, Austin, TX 78712

E. L. van Dessel: Royal Belgian Observatory, Ringlaan 3, 1080 Brussel, Belgium

M. Watson: Physics Dept., University of Leicester, Leicester, England